# COMPLEMENTARY SPLIT RING RESONATORS WITH DUAL MESH-SHAPED COUPLINGS AND DEFECTED GROUND STRUCTURES FOR WIDE PASS-BAND AND STOP-BAND BPF DESIGN

**J. C. Liu and H. C. Lin**

Department of Electrical Engineering
Ching Yun University
Chung-Li, Tao-yuan 32097, Taiwan, R.O.C.

**B. H. Zeng**

Department of Communication Engineering
Yuan Ze University
Chung-Li, Tao-yuan 32003, Taiwan, R.O.C.

**Abstract**—Novel configurations of complementary split ring resonator (CSRR) with dual mesh-shaped couplings and defected ground structures (DGS) are introduced to design the high performance of wide pass-band and stop-band band pass filters (BPF). This paper presents a low insertion loss ($-0.82$ dB), symmetry and sharper transmission zero level ($-51.88$ dB), using effective DGS and alternative coupling for CSRR. The filter with center frequency at 1.92 GHz, pass-band from 1.21 GHz to 3.05 GHz (BW = 95.8%) and wider stop-band (extended to $4.2f_0$ below $-20$ dB rejection level) is designed and fabricated. Simulation and measured results including surface current distributions and frequency responses are presented and discussed.

## 1. INTRODUCTION

The attractive features of the microstrip ring resonator are its compact size, low cost, high $Q$ and low radiation loss. In applications, the ring resonator has been used to design filters, mixers, oscillators and antennas [1]. Recently, the novel double slot ring resonators, named complementary split-ring resonators (CSRR), were developed for band

---

pass filter [2–11], band reject filter [12], low pass filter [13] and high pass filter [14] applications. Basically, these filters based on CSRR structure and alternative couplings were used to design the desired filter for applications.

Dual mesh-shaped coupling applied in configurations of CSRR, designated as CSRR-based BPF, are constructed. First, the novel dual mesh-shaped coupling is used to present the coupling way in wide pass-band applications. To obtain a good performance with wide stop-band, an improved CSRR with DGS [15–17] are proposed and compared then. Simulation results including surface current distributions and frequency responses are presented and discussed.

## 2. FILTER CONFIGURATIONS AND BASIS

CSRR-based BPF consisted with CSRR and DGS structure etched on the ground and the couplings located on the top of the microstrip are presented in Fig. 1. The dual mesh-shaped coupling is depicted in Fig. 1(a), the physical dimensions are stated: $a_1 = 0.45\,\text{mm}$, $a_2 = 0.1\,\text{mm}$, $a_3 = 7.6\,\text{mm}$, $b_1 = 2.6\,\text{mm}$, $b_2 = 3\,\text{mm}$, $b_3 = 5.5\,\text{mm}$, $c_1 = 0.4\,\text{mm}$, $c_2 = 0.2\,\text{mm}$. The CSRR configuration on the bottom of the microstrip is presented in Fig. 1(b) with dimensions as: $L = 23.5\,\text{mm}$, $W = 17\,\text{mm}$, $R_1 = 5.2\,\text{mm}$, $R_2 = 3.55\,\text{mm}$, $G_1 = 1.6\,\text{mm}$, $G_2 = 1.1\,\text{mm}$, $G_3 = 0.6\,\text{mm}$. The CSRR and DGS configuration on the bottom of the microstrip is presented in Fig. 1(c) with dimensions as: $G_4 = 5.72\,\text{mm}$, $s_1 = 5\,\text{mm}$, $s_2 = 2.7\,\text{mm}$, $s_3 = 2.35\,\text{mm}$, $s_4 = 1\,\text{mm}$, $s_5 = 0.6\,\text{mm}$, $g = 0.3\,\text{mm}$.
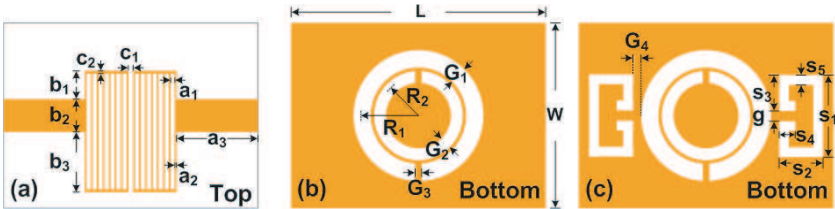


**Figure 1.** CSRR-based BPF. (a) Mesh-shaped coupling, (b) CSRR, (c) CSRR and DGS.

## 3. SIMULATIONS AND RESULTS

The simulations for the CSRR-based band pass filter are achieved with the aid of CAD IE3D [18]. The FR4 substrate with dielectric constant $\varepsilon_r = 4.4$, thickness $h = 0.4\,\text{mm}$ is used for experiments. For the

requirement of $50\,\Omega$ impedance, the width of strip is $3\,\text{mm}$, length of feed-line is $7.6\,\text{mm}$, effective dielectric constant $\varepsilon_{eff} = 2.61$ and guided wavelength $\lambda_g = 96.71\,\text{mm}$ at frequency $f_0 = 1.92\,\text{GHz}$.

### 3.1. Frequency Responses

For practice, the simulated and measured $S_{21}$ and $S_{11}$ frequency responses of the band pass filter are shown in Fig. 2 and Fig. 3. Both the simulations and measurements are with good agreement. For simulation results, the performance with lower insertion loss $(-0.85\,\text{dB})$, deeper transmission zero level $(-52.36\,\text{dB})$ and wider bandwidth $(\text{BW} = 96\%)$ at the central frequency $1.91\,\text{GHz}$ are obtained for CSRR BPF. In addition, the lower insertion loss $(-0.82\,\text{dB})$, symmetry and deeper transmission zero level $(-51.88\,\text{dB})$, wider bandwidth $(\text{BW} = 95.8\%)$ and wider stop-band (extended to $4.2f_0$ below $-20\,\text{dB}$ rejection level) at the central frequency $1.92\,\text{GHz}$ are obtained for CSRR and DGS BPF respectively. The performances of the filter are listed in Table 1.

**Table 1.** CSRR with dual mesh-shaped couplings and DGS results.

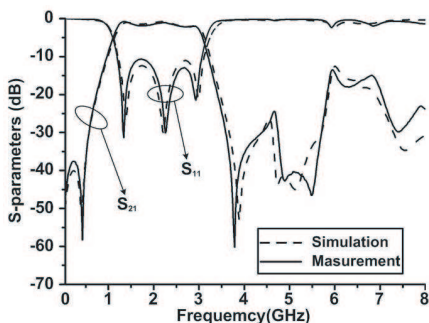| Pass band | | | Stop band | |
| --- | --- | --- | --- | --- |
| $f_0$ (GHz) | | 1.92 | At $2.45f_0$ (dB) | $-38.39$ (deep) |
| $-3\,\text{dB BW}$ (GHz) | | 1.84 | At $2.82f_0$ (dB) | $-45.55$ (deep) |
| FBW (%) | | 95.8 | At $3.84f_0$ (dB) | $-41.50$ (deep) |
| Min insertion loss (dB) | | $-0.82$ | To $4.16f_0$ (dB) | Below $-20.00$ |
| Zero level (dB) | Lower | $-51.88$ | - | - |
| | Upper | $-36.45$ | | |



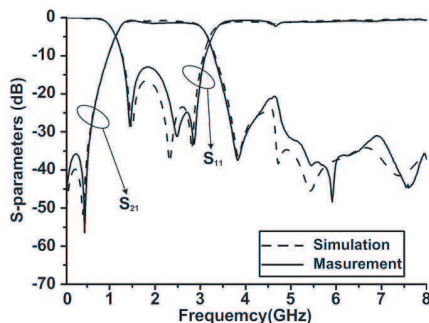**Figure 2.** Simulation and measurement results of CSRR BPF.



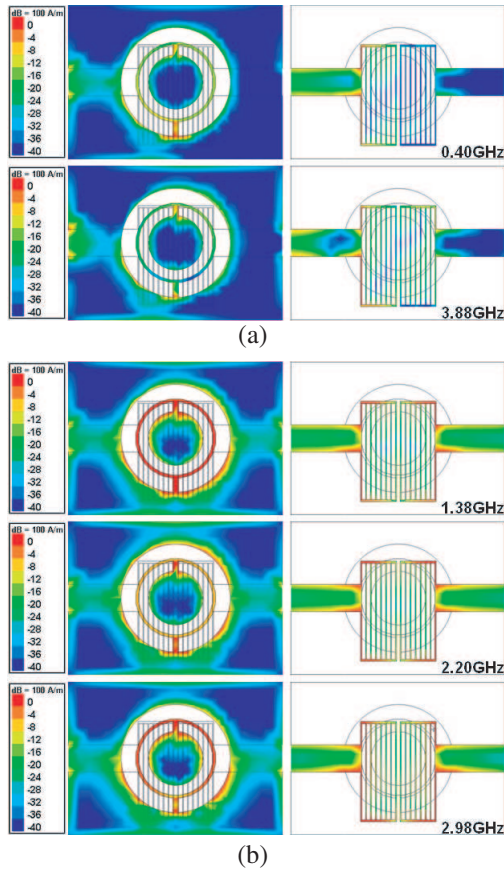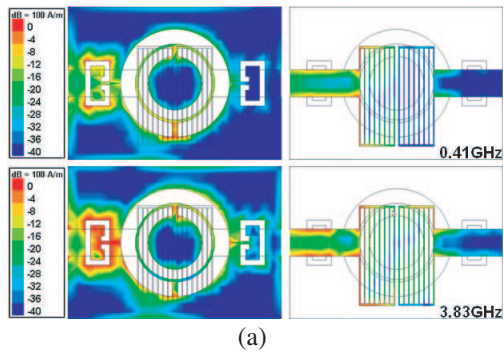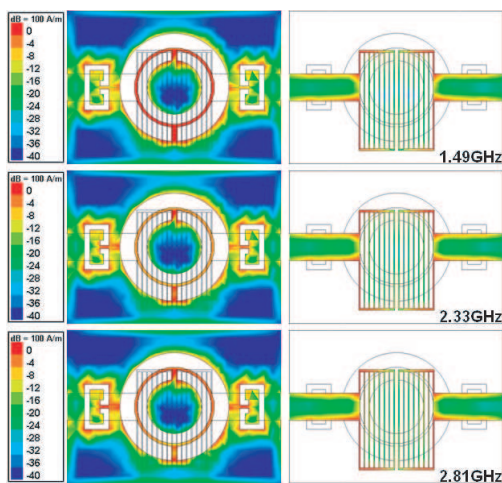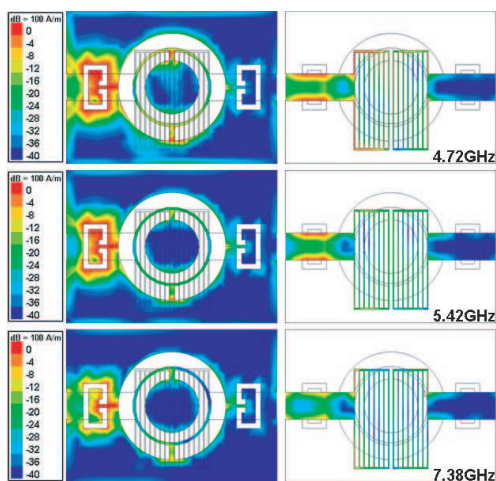**Figure 3.** Simulation and measurement results of CSRR and DGS BPF.

**Figure 4.** Current distributions of CSRR BPF. (a) Two zeros, (b) three resonances.

(b)



(c)

**Figure 5.** Current distributions of CSRR and DGS BPF. (a) Two zeros, (b) three resonances, (c) three deep resonances.

## 3.2. Surface Current Distributions

Among the band pass filter with CSRR and dual mesh-shaped coupling structures, results in Fig. 4 and Fig. 5 present the surface current distributions simulated by IE3D. The CSRR exhibits the blue surface current distributions at two transmission zeros at 0.40 and 3.88 GHz

and the dual mesh-shaped coupling presents the lower couplings at the transmission zeros in Fig. 4(a). Meantime, the CSRR exhibits the heavy surface current distributions at the resonances 1.38, 2.20 and 2.98 GHz and the dual mesh-shaped coupling presents the higher couplings at these resonated frequencies Fig. 4(b).

On the second example, the CSRR exhibits the blue surface current distributions at the transmission zeros at 0.41 and 3.83 GHz and the dual mesh-shaped coupling presents the lower couplings at the transmission zeros in Fig. 5(a). Meantime, the CSRR exhibits the heavy surface current distributions at the resonances 1.49, 2.33 and 2.81 GHz and the dual mesh-shaped coupling presents the higher couplings at the resonated frequencies in Fig. 5(b). Obviously, three deep resonances at $2.45f_0$, $2.82f_0$ and $3.84f_0$ within stop-band are presented in Fig. 5(c). The heavy surface current distributions are fully sunk in the DGS structure.

## 3.3. Mesh-shaped Coupling Variations

The variations of mesh-shaped couplings with CSRR are shown in Fig. 6. The mesh number with $n = 0, 2, 4, 6$ and 8 for mesh are studied for optimization. When the values of $b_1/b_3$ increases, the rejection decreases gradually and the response symmetry as well as flatness increases, while $n = 0$ keep constant. Whereas the number $n$ increases, the rejection decreases and the response flatness increases, while $b_1/b_3 = 0.47$. In the case of mesh number $n = 6$ and $b_1/b_3 = 0.47$, the CSRR based BPF can be available for design. The frequency responses are presented in Fig. 7. The performance is listed in Table 2. The photograph of the CSRR based BPF is presented in Fig. 8.

**Table 2.** Mesh sheped coupling results.

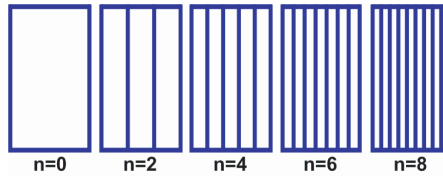| Simulation | | $n = 0$ | $n = 2$ | $n = 4$ | $n = 6$ | $n = 8$ |
|---|---|---|---|---|---|---|
| $f_0$ (GHz) | | 2.53 | 2.17 | 2.01 | 1.91 | 1.87 |
| $-3\,\text{dB BW (GHz)}$ | | 1.77 | 1.90 | 1.88 | 1.81 | 1.83 |
| FBW (%) | | 69.9 | 87.5 | 93.5 | 96 | 97.8 |
| Min insertion loss (dB) | | $-1.30$ | $-0.99$ | $-0.89$ | $-0.85$ | $-0.83$ |
| Zero Level | Lower | $-51.01$ | $-52.48$ | $-51.88$ | $-51.95$ | $-51.42$ |
| (dB) | Upper | $-46.18$ | $-50.07$ | $-52.20$ | $-52.36$ | $-54.73$ |

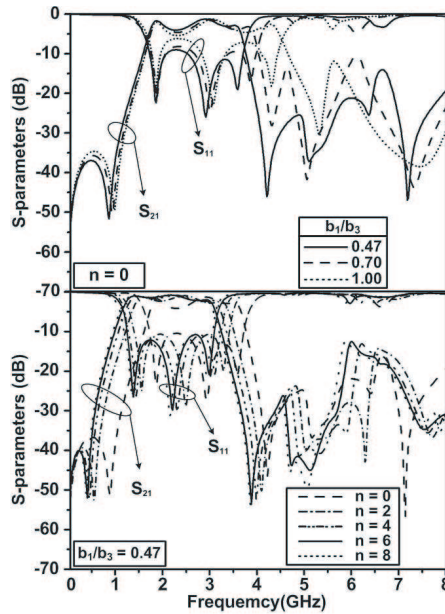**Figure 6.** Mesh-shaped coupling variations.



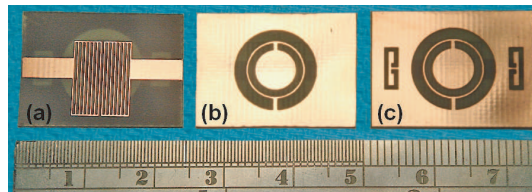**Figure 7.** Simulation results of mesh-shaped coupling variations.



**Figure 8.** Photograph of high pass filter. (a) Dual mesh-shaped coupling, (b) CSRR, (c) CSRR and DGS.

## 4. CONCLUSIONS

The novel configurations of CSRR with dual mesh-shaped couplings and DGS are introduced to design the high performance of BPF. For comparison, two CSRR-based BPF with dual mesh-shaped coupling and/or DGS are studied. To obtain lower insertion loss ($-0.82$ dB), symmetry and deeper transmission zero level ($-51.88$ dB), wider bandwidth (BW $= 95.8\%$) and wider stop-band (extended to $4.2 f_0$ below $-20$ dB rejection level) at the central frequency $1.92$ GHz of the pass-band and stop-band filter are presented.

These filters can achieve the wide pass-band and the good stop-band. Its coupling way is efficient. The structure is smaller in size and easy to fabricate. It can be applied to the UWB and microwave systems.

## REFERENCES

1. Chang, K., *Microwave Ring Circuits and Antennas*, John Wiley, New York, 1996.

2. Bonache, J., F. Martin, J. Garcia, I. Gil, and R. Marques, "Ultra wide band pass filters (UWBPF) based on complementary split rings resonators," *Microwave Opt. Tech. Lett.*, Vol. 46, No. 3, 283–286, Aug. 2005.

3. Bonache, J., F. Martin, F. Falcone, J. D. Baena, T. Lopetegi, J. Garcia, M. A. G. Laso, I. Gil, A. Marcotegui, R. Marques, and M. Sorolla, "Application of complementary split-ring resonators to the design of compact narrow band-pass structures in microstrip technology," *Microwave Opt. Tech. Lett.*, Vol. 46, No. 5, 508–512, Sep. 2005.

4. Baena, J. D., J. Bonache, F. Martin, R. M. Sillero, F. Falcone, T. Lopetegi, M. A. G. Laso, J. Garcia, I. Gil, M. F. Portillo, and M. Sorolla, "Equivalent-circuit models for split-ring resonators and complementary split-ring resonators coupled to planar transmission lines," *IEEE Trans. Microwave Theory and Tech.*, Vol. 53, No. 4, 1451–1461, Apr. 2005.

5. Bonache, J., I. Gil, J. Garcia, and F. Martin, "Novel microstrip bandpass filters based on complementary split-ring resonators," *IEEE Trans. Microwave Theory and Tech.*, Vol. 54, No. 11, 265–271, Jan. 2006.

6. Mondal, P., M. K. Mandal, A. Chaktabarty, and S. Sanyal, "Compact bandpass filters with wide controllable fractional

bandwidth," *IEEE Microw. Wireless Compon. Lett.*, Vol. 16, No. 10, 540–542, Oct. 2006.

7. Wu, H. W., Y. K. Su, M. H. Weng, and C. Y. Hung, "A compact narrow-band microstrip bandpass filter with a complementary split-ring resonator," *Microwave Opt. Tech. Lett.*, Vol. 48, No. 10, 2103–2106, Oct. 2006.

8. Wu, H. W., M. H. Wang, Y. K. Su, R. Y. Yang, and C. Y. Hung, "Accurate equivalent circuit for etched resonator with effective negative permittivity," *Microwave Opt. Tech. Lett.*, Vol. 49, No. 1, 231–234, Jan. 2007.

9. Wu, H. W., M. H. Wang, Y. K. Su, R. Y. Yang, and C. Y. Hung, "Propagation characteristics of complementary split-ring resonator for wide bandgap enhancement in microstrip bandpass filter," *Microwave Opt. Tech. Lett.*, Vol. 49, No. 2, 292–295, Feb. 2007.

10. Zhang, X. C., Z. Y. Yu, and J. Xu, "Novel band-pass substrate integrated waveguide (SIW) filter based on complementary split ring resonators (CSRRS)," *Progress In Electromagnetics Research*, PIER 72, 39–46, 2007.

11. Wu, G. L., W. Mu, X. W. Dai, and Y. C. Jiao, "Design of novel dual-band bandpass filter with microstrip meander-loop resonator and CSRR DGS," *Progress In Electromagnetics Research*, PIER 78, 17–24, 2008.

12. Garcia, J., F. Martin, F. Falcone, J. Bonache, J. D. Baena, I. Gil, E. Amat, T. Lopetegi, M. A. G. Laso, J. A. M. Iturmendi, M. Sorolla, and R. Marques, "Microwave filters with improved stopband based on sub-wavelength resonators," *IEEE Trans. Microwave Theory and Tech.*, Vol. 53, No. 6, 1997–2006, Jun. 2005.

13. Zhang, J., B. Cui, S. Lin, and X.-W. Sun, "Sharp-rejection low-pass filter with controllable transmission zero using complementary split ring resonators (CSRRS)," *Progress In Electromagnetics Research*, PIER 69, 219–226, 2007.

14. Niu, J. X. and X. L. Zhou, "Analysis of balanced composite right/left handed structure based on different dimensions of complementary split ring resonators," *Progress In Electromagnetics Research*, PIER 74, 341–351, 2007.

15. Shi, J., J. X. Chen, and Q. Xue, "A quasi-elliptic function dual-band bandpass filter stacking spiral-shaped cpw defected ground structure and back-side coupled strip lines," *IEEE Microw. Wireless Compon. Lett.*, Vol. 17, No. 6, 430–432, Jun. 2007.

16. Maddah-Ali, M., H. D. Oskouei, and K. Forooraghi, "A compact

branch-line coupler using defected ground structures," *Microwave Opt. Tech. Lett.*, Vol. 50, No. 6, 386–389, Feb. 2008.

17. Kuan, H. and H. Y. Pan, "Design of a dual-mode bandpass filter with wide stopband performance for GPS application," *Microwave Opt. Tech. Lett.*, Vol. 50, No. 6, 445–447, Feb. 2008.

18. Zeland Software Inc., IE3D version 10.0, Jan. 2005.